

PAPER • OPEN ACCESS

## Theoretical and experimental researches of the liquid evaporation during thermal vacuum influences

To cite this article: V Trushlyakov *et al* 2018 *J. Phys.: Conf. Ser.* **944** 012119

View the [article online](#) for updates and enhancements.

You may also like

- [Innovation of Cooking Juice in Process Production of Red-Cane Sugar in Lawang Village of Agam District](#)  
Firdaus, E Praputri, E Sundari et al.
- [Evaporation characteristics of ethanol droplet in different gases under force convection condition](#)  
Numan Siddique Mazumder, Pradip Lingfa and Champak Kr Neog
- [A combined MEMS thermal vacuum sensor with a wide pressure range](#)  
Chuang Yuan, Jianyu Fu, Fan Qu et al.



**ECS**  
The  
Electrochemical  
Society  
Advancing solid state &  
electrochemical science & technology

**DISCOVER**  
how sustainability  
intersects with  
electrochemistry & solid  
state science research

# Theoretical and experimental researches of the liquid evaporation during thermal vacuum influences

V Trushlyakov<sup>1</sup>, A Panichkin<sup>2</sup>, O Prusova<sup>1</sup>, K Zharikov<sup>1</sup> and M Dron<sup>1</sup>

<sup>1</sup>Omsk State Technical University, 11, Mira ave., Omsk, 644050, Russia

<sup>2</sup>Institute of mathematics n. a. S. Sobolev SB RAS, Novosibirsk, Russia

e-mail: [olga.prusova@mail.ru](mailto:olga.prusova@mail.ru)

**Abstract.** The mathematical model of the evaporation process of model liquid with the free surface boundary conditions of the "mirror" type under thermal vacuum influence and the numerical estimates of the evaporation process parameters are developed. An experimental stand, comprising a vacuum chamber, an experimental model tank with a heating element is designed; the experimental data are obtained. A comparative analysis of numerical and experimental results showed their close match.

## 1. Introduction

The method of thermal vacuum drying is widely used in various industries, for example, in [1, 2] a method and a device for thermal vacuum drying of wet particulate materials are described. Heating of the raw materials occurs in a reservoir in which thermally insulated space between the walls a resistive heater is placed. In [3–6], the methods of vacuum drying and a device for vacuum drying used in food, medical, microbiological and chemical industries are described. Heating of the dried product takes place on the heated shelves of the heating elements unit. In [3–5], conductive heating of the heated shelves is carried out. In [6] heating elements have an internal cavity forming a reservoir inlet and outlet of the hot heat carrier.

However, these methods are only used for the dehydration of porous and particulate materials. In [7], to dry the internal cavity of the pipeline to the required moisture content, initial vacuuming and then blowing the pipeline with pre-drained gas is suggested. In [8], for drying the pipeline, the cavity is pre-evacuated to a pressure of 0.2 to 0.005 kgf/cm<sup>2</sup>, and then, maintaining the achieved vacuum, water vapour is pumped from the cavity of the pipeline until complete evaporation of the water film. Final drying to the required residual moisture content takes place with venting the cavity gas, which drying is carried out by its extensions inside the drained cavity due to the vacuum maintained there.

In [9, 10], the results of numerical studies of the influence of various parameters such as initial temperature, pressure, density and drop diameter, specific heat and thermal conductivity, and pressure in the vacuum chamber on the process of drops vacuum freeze are presented. The estimation of these parameters impact on the processes of drops cooling and freezing is presented. It is noted that the process of mass transfer at the droplet surface is different for the micro droplets (<100 μm) and macro droplets (>1 mm).

In [11, 12], the results of experimental and theoretical studies of the evaporation – freezing a pendent water drop in the conditions of deep vacuum are described.



As it can be seen from the above, the drying process of reservoirs and pipelines via vacuum by evaporation of the water film is widely used nowadays. However, theoretical and experimental studies were carried out only for a single drop of liquid. Below is a discussion of theoretical and experimental studies of the evaporation process from the surface layer of the model liquid (ML) on the example of water for boundary conditions of «mirror» type (water film) under the conditions of decompression and thermal loading. The efficiency of the evaporation process is proposed to evaluate the ratio of the evaporated ML mass and the energy spent on evaporation.

## 2. Statement of the research problem

The study of the ML evaporation process, in an experimental model tank (EMT) under reduced pressure in a vacuum chamber (VC) and temperature effects, involves the following physical-mathematical model.

At the initial moment  $t_0$  ML, volume  $V_w$  and temperature  $T_w$ , in the EMT, is placed in the VC volume  $V_v$  and the air temperature  $T_v$  with the boundary position of the free surface of ML in the form of a "mirror" area of  $S_0$ . EMT has a form of a tub (figure 2) with mass  $m_s$  (volume  $V_s$ , density  $\rho_s$ ) for the ML placement and the possibility of the ML heating. The initial pressure in the VC is atmospheric  $P_a$  with the partial pressure of water vapour  $P_p$  in the corresponding mass of dry air  $m_a$  and model liquid  $m_p$ . Pumping air from the VC is given as a continuous function of the volume  $dV$  element during the time  $dt$ .

In the process of air pumping with a pumping rate of  $dV/dt$  from time  $t_1$  to  $t_2 = t_1 + dt$  with its volume increased from  $V_1$  to  $V_2 = V_1 + dV$  simultaneous decrease in the pressure from  $P_1$  to  $P_2$ , and temperature from  $T_1$  to  $T_2$  and the density from  $\rho_{v1}$  to  $\rho_{v2}$  will occur. It is assumed that the share of pumped air volume  $dV$  gets the same changes of parameters like the volume of air  $V_v$  remaining in the VC, i.e.:

$$P_2 = P_1 - dP; T_2 = T_1 - dT; \rho_{v2} = \rho_{v1} - d\rho_v.$$

The density of the mixture of dry air with the mass  $m_a$  and water vapour with the mass  $m_p$  is defined as:

$$\rho_v = (m_a + m_p) / V_v, \quad (1)$$

where VC volume  $V_v$  is constant in time, and  $V_1 = V_v$ .

During weak external and internal heat transfer, the process of pumping can be considered adiabatic with ratio of specific heats for the air and water vapour  $k=1.4$ , so, for this process the following formula is valid [13]

$$P_1 V_1^k = P_2 V_2^k = (P_1 - dP)(V_1 + dV)^k = const; \quad (2)$$

$$T_1 V_1^{k-1} = T_2 V_2^{k-1} = (T_1 - dT)(V_1 + dV)^{k-1} = const. \quad (3)$$

In the process of ML evaporation from  $t_1$  to  $t_2 = t_1 + dt$  with a rate of  $dm_p/dt$  on the value of  $dm_p$  the pressure in the VC reaches:

$$P_2 = \left( \frac{m_a}{\mu_a} + \frac{m_p + dm_p}{\mu_p} \right) R_0 T_2 / V_2, \quad (4)$$

where  $R_0 = 8.314 \text{ J}/(\text{mole} \cdot \text{K})$  – is gas constant;  $\mu_a = 0.02897 \text{ kg}/\text{mole}$  and  $\mu_p = 0.01802 \text{ kg}/\text{mole}$  – is the molar mass of dry air and water vapour. The temperature and pressure in (4) are related by

$$T_1^k / T_2^k = P_1^{k-1} / P_2^{k-1} = const, \quad (5)$$

from which and from (3) the temperature is determined:

$$T_2 = T_1 + dT = \left[ \left( \frac{m_a}{\mu_a} + \frac{m_p + dm_p}{\mu_p} \right) R_0 / (V_1 + dV_2) \right]^{k-1} T_1^k / P_1^{k-1} \quad (6)$$

with the subsequent substitution in (4) for determining  $P_2$ .

Density (1) at time  $t_1$  with a mass of dry air and a vapour of ML for time  $t_2$  will be

$$\rho_{v2} = (m_{a1} + m_{p1} + dm_p) / (V_1 + dV), \quad (7)$$

from where the mass  $m_a$  of dry air and vapour ML  $m_p$  at time  $t_2$ , remaining in the volume  $V_V$  VC will follow

$$m_{a2} = m_{a1} V_V / (V_V + dV); \quad m_{p2} = (m_{p1} + dm_p) V_V / (V_V + dV). \quad (8)$$

To simulate the process of ML evaporation at the boundary with air, the dependences on temperature and pressure, and other parameters characterizing the liquid and the air, are used. It is known, for example, that the dependence of the evaporation rate from the surface  $S$  on the liquid temperature  $T_w$  is given by [13, 14]

$$W_w(T_w) = V_w(T_0) \cdot \exp\left(\frac{LM(T_w - T_0)}{RT_w T_0}\right), \quad (9)$$

where  $T_0$  – is the freezing temperature (K);  $M$  – is the molar mass of liquid (kg/mole);  $L$  – is the specific heat of vaporization (J/kg);  $R_0$  – universal gas constant (J/(kg·K)).

To simulate the evaporation rate from unit area  $W_s$  (kg/(m<sup>2</sup>·s)) the formula in the following form is used

$$W_w(P, T_w) = K_1 \cdot (P_w(T_w) - P_d) \left(\frac{P_0}{P}\right)^q, \quad (10)$$

where  $K_1$  is the coefficient of condition of the ML evaporated surface (the still «mirror» type or undulating) and the movement of air (kg/(Pa·m<sup>2</sup>·s));  $P_w$  is the partial pressure of evaporated ML saturation at its current temperature  $T_w$  (Pa);  $P_d$  is the partial pressure of mg vapour in air (Pa);  $P_0$  is the initial atmospheric pressure (Pa);  $P$  is the current pressure in the VC (Pa);  $q$  is the linearity for the given ML (0.66÷1.18).

For still air in the VC the  $K_1$  value, in accordance with [15], is taken equal to  $1.39 \cdot 10^{-9}$  kg/(Pa·m<sup>2</sup>·s).

To account for the condensation of ML the rate formula similar to (10), with partial saturation pressure  $P_v$  under the air temperature  $T_v$ , is considered

$$W_v(P, T_v) = K_1 (P_v(T_v) - P_d) \left(\frac{P_0}{P}\right)^q. \quad (11)$$

The VC will be considered in the following regions (figure 1):  $W_0$  – EMT;  $W_1$  is the region of the liquid film in the EMT;  $W_2$  is the air environment in the VC;  $W_3$  is the VC wall. Between these regions heat and mass transfer will be modelled with the given parameters, such as the mass  $m_i$ , the heat capacity  $C_{pi}$ , the thermal conductivity  $\lambda_i$ , the density  $\rho_i$  ( $i = 0, 1, 2, 3$  for base coat, liquid, air and the case wall of VC respectively) and the initial temperatures  $T_s$ ,  $T_w$ ,  $T_v$ ,  $T_k$ .

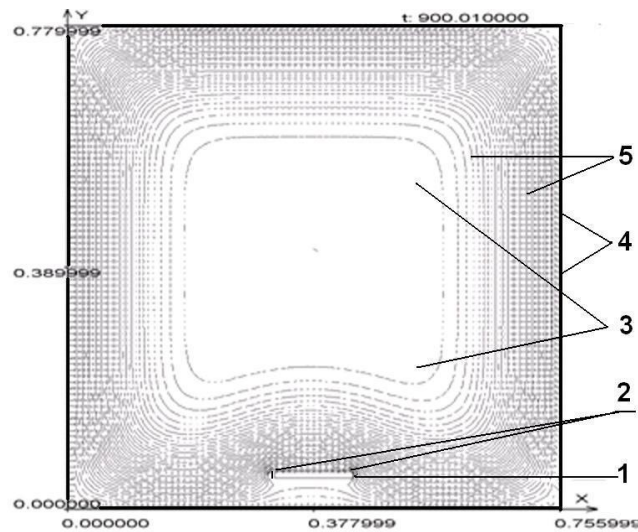


**Figure 1.** The region of numerical modelling in the VC with the temperature distribution at time  $t = 900$  s: 1 – the EMT ( $W_0$ ); 2 – the film (mirror) of the liquid ( $W_1$ ); 3 – the air ( $W_2$ ); 4 – the VC case wall ( $W_3$ ); 5 – the contours of temperature (*in the preliminary estimates at this stage of the research the air velocity and liquid was not considered because of their smallness*).

We assume that at the initial moment  $t_0 = 0$  in the VC and outside it the preset atmospheric pressure  $P_0 = 101323.2$  Pa with a certain ML moisture percentage

$$C_1 = 100 \cdot (P_{pn} - P_p) / P_{pn}, \quad (12)$$

where  $P_{pn}(T_V)$  is the partial pressure of saturated air at liquid;  $P_p = (m_p / \mu_p) R_0 T_V / V_V$  is the partial vapour pressure of ML in the air;  $m_p$  is the mass of the liquid vapour in the air;  $\mu_p = 0.01802$  kg/mole is the molar mass of the vapour;  $R_0 = 8.314$  J/(mole·K) is the universal gas constant.

The value of  $P_{pn}(T_V)$  is tabular and at  $T_V = 20$  °C is equal to 2338.43 Pa.

Consequently, we formulate the initial-boundary value problem of evaporation of a viscous incompressible heat-conducting fluid from the EMT and pumping of viscous heat-conducting air from the rectangular region with the wall thickness  $h$ , the length  $L_0$  as a two-dimensional problem.

### 3. Equations of heat transfer

We will consider two-dimensional problem in one section of the VC, given the size of the EMT width, with defined boundary conditions under the velocity of the air  $\Delta V_V$  ( $m^3/s$ ) and a decrease in the internal air pressure  $P_V$  and temperature  $T_V$  according to the equations (4) – (6).

For numerical simulation of heat transfer in each of the regions  $W_0$ ,  $W_1$ ,  $W_2$ ,  $W_3$  the equation of heat transfer for a particular environment (air, liquid, solid) will have the following form [13]:

$$\frac{\partial T}{\partial t} + (\mathbf{V} \cdot \nabla) T = \lambda \nabla^2 T, \quad (13)$$

where  $\mathbf{V} = \mathbf{V}(u, v)$  – is the velocity vector of the moving environment (for air and liquid);  $T$  – is the environment temperature;  $\lambda$  – is the thermal diffusivity ( $K = \lambda C_p \rho$  – is the conductivity).

For the simulation of heat and mass transfer let us define the region sizes in metres:  $W_0 = [0.372, 0.384] \times [0.050, 0.052]$ ;  $W_1 = [0.372, 0.384] \times [0.052, 0.053]$ ;  $W_2 = [0.018, 0.738] \times [0.018, 0.762]$  –  $W_0 - W_1$ ;  $W_3 = [0.000, 0.756] \times [0.000, 0.780]$  –  $W_0 - W_1 - W_2$ .

For the heat equation (13), the conditions of heat fluxes conservation from some regions to others [13] are used.

We indicate the VC size on the x-axis:  $x_0 = 0$  m,  $x_1 = 0.018$  m,  $x_2 = 0.372$  m,  $x_3 = 0.384$  m,  $x_4 = 0.738$  m,  $x_5 = 0.756$  m; the size on the y-axis:  $y_0 = 0$  m,  $y_1 = 0.018$  m,  $y_2 = 0.050$  m,  $y_3 = 0.052$  m,  $y_4 = 0.053$  m,  $y_5 = 0.762$  m,  $y_6 = 0.780$  m.

On the boundary  $W_0$ ,  $W_1$ ,  $W_2$ , having respective coefficients heat conductivity  $K_0=\lambda_0 C_{p0} \rho_0$ ,  $K_1=\lambda_1 C_{p1} \rho_1$ ,  $K_2=\lambda_2 C_{p2} \rho_2$ , between themselves, we shall take into account the conservation of heat fluxes in the form:

$$K_2 \frac{\partial T}{\partial y}(x, y_2^-) = K_0 \frac{\partial T}{\partial y}(x, y_1^+), \quad K_0 \frac{\partial T}{\partial y}(x, y_3^-) = K_1 \frac{\partial T}{\partial y}(x, y_3^+),$$

$$K_1 \frac{\partial T}{\partial t}(x, y_4^-) = K_2 \frac{\partial T}{\partial y}(x, y_4^+), \quad x_2 \leq x \leq x_3, \quad (14)$$

On the boundary of the region  $W_2$  with the heat-conducting VC case with a coefficient of thermal conductivity  $K_3=\lambda_3 C_{p3} \rho_3$  for  $T$  accepts the following conditions, similar to (14), are accepted:

$$K_3 \frac{\partial T}{\partial x}(x_1^-, y) = K_2 \frac{\partial T}{\partial x}(x_1^+, y), \quad K_2 \frac{\partial T}{\partial x}(x_4^-, y) = K_3 \frac{\partial T}{\partial x}(x_4^+, y), \quad y_1 \leq y \leq y_5,$$

$$T'_x(x, 0^+) = 0, \quad T'_x(x, y_6^-) = 0, \quad x_0 \leq x \leq x_5,$$

$$T'_x(0^+, y) = 0, \quad T'_x(x_5^-, y) = 0, \quad y_0 \leq y \leq y_6. \quad (15)$$

At the initial time  $t = 0$  are specified: the temperature in all the calculated regions and the air pressure from the partial vapour pressure of ML further based on the time interval  $[0, t^*]$  to the critical point  $t^*$ , when the ML freezing will occur (in the mathematical model the process of ML freezing is not used).

#### 4. Experimental studies

1. Preparatory experiments are the following:

- Testing of experimental stand measuring complex (temperature and pressure sensors);
- Testing of the vacuum creation system (vacuum pump, pneumatic valves, connectors and valves, pressure sensor);
- Testing of individual elements of the experiments programme (the evaporation time of a given mass of model liquid, etc.).

2. The main experiments in the VC are the following:

- The evaporation time measurement of a given mass of ML with heating and without heating;
- The ML mass before and after the experiment;
- The ML temperature measurement, in the EMT, gas-vapour mixture and pressure in the VC.

Figure 2 presents a schematic structural diagram of experimental stand for the research of ML evaporation under thermal vacuum influences.

The measured parameters of ML evaporation process are:

- The ML temperature (K);
- The pressure in the VC (Pa);
- The evaporation time (sec);
- The power used for evaporation of a given ML mass (W).

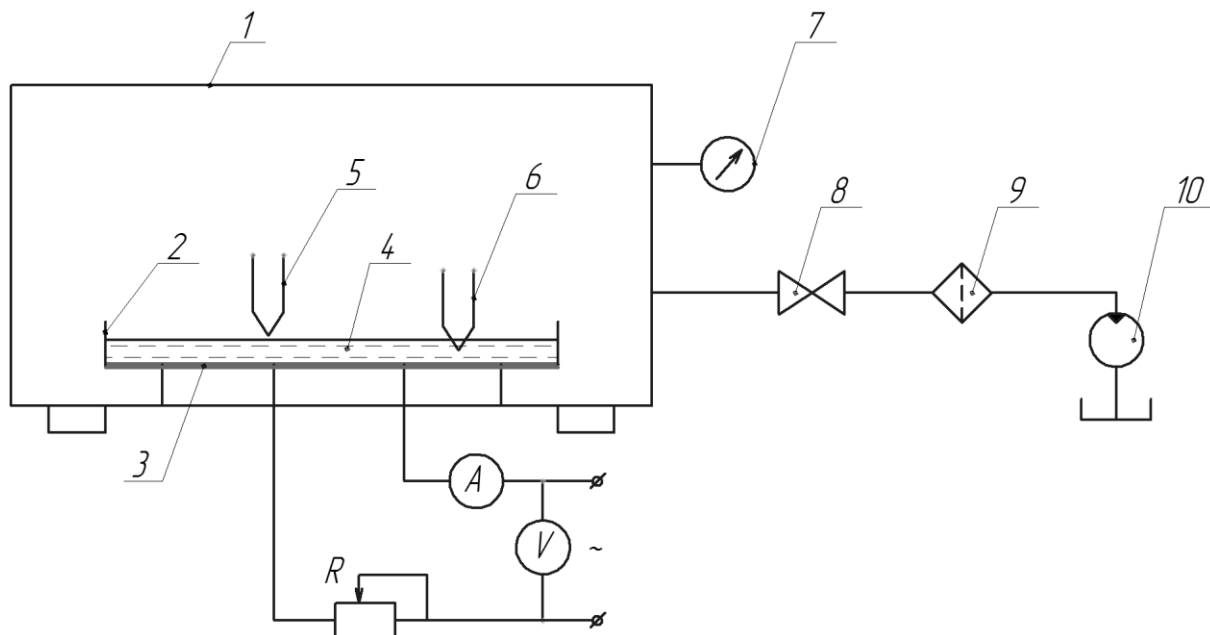


**Figure 2.** The experimental stand vacuum scheme: 1 – the vacuum chamber; 2 – the EMT; 3 – the heating element; 4 – the ML; 5, 6 – the thermocouples; 7 – the pressure sensor; 8 – the valve; 9 – the filter; 10 – the vacuum pump.

## 5. The test calculation results

Numerical calculations were carried out in accordance with (12) – (15) including evacuating air from the VC volume  $V_v = 0.463 \text{ m}^3$  with a velocity of  $dV/dt = 0.0065 \text{ m}^3/\text{s}$  when using the ML evaporation model according to the formulas (10) – (11) and the model of gas-dynamic quantities in equations (1) – (8) change.

In the formula (10) for the boundary conditions of the ML evaporable surface "mirror the coefficient  $K_1 = 1.39 \cdot 10^{-8} \text{ kg}/(\text{Pa} \cdot \text{m}^2 \cdot \text{s})$  and linearity  $q = 1.18$ " were used.

The calculation of heat transfer parameters in equations (13) – (15) with the use of algorithms based on economical difference schemes [16] was carried out.

Based on the developed software product [16] numerical modelling of heat and mass transfer with ML evaporation surface in the process of reducing atmospheric pressure in the VC was carried out.

When using a computational grid with  $N_x = 80$  and  $N_y = 80$  the test calculation of the three options for the ML evaporation in the VC with the amount of ML = 5.0 ml, 10.0 ml and 20.0 ml, which constituted the initial levels of liquid in the tub is 0.2 mm, 0.4 mm and 0.8 mm, respectively, was made.

Fig. 1 shows the picture of isolines of the temperature characteristic of the heat transfer with a volume of 20.0 ml at a pumping rate  $V_1 = 6.5 \text{ l/s}$  and time of 900 s.

The calculations for these three options with the ML amount 5.0 ml, 10.0 ml and 20.0 ml without heating was carried out up to time 360 s, 600 s and 900 s, respectively. For the given time points, the level of ML ( $h$ ) and temperature ( $T$ ) with an initial moisture content of 0% in the chamber was made up of the following values:

- $h$ : 0.094 mm, 0.140 mm, 0.223 mm;
- $T$ : 270.9 K, 271.2 K, 271.4 K.

Similar data were obtained for a moisture content of 100% in-chamber:

- $h$ : 0.097 mm, 0.143 mm, 0.226 mm;
- $T$ : 271.3 K, 271.6 K, 271.6 K,

This indicates greater ML evaporation at a lower initial moisture content in VC.

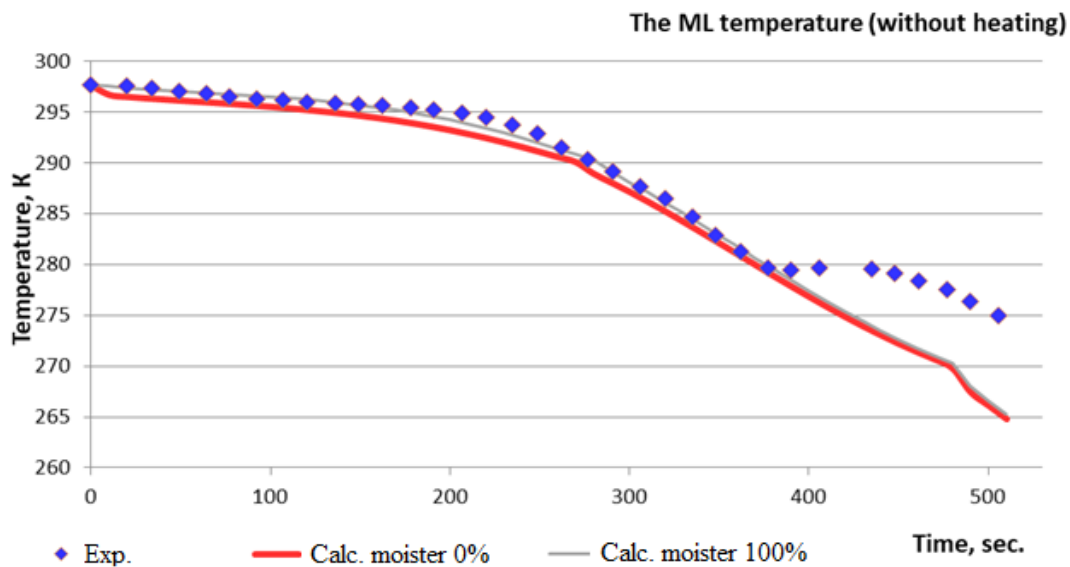
## 6. Comparison of numerical and experimental results

In the course of the calculations and experiments the following dependence of ML temperature

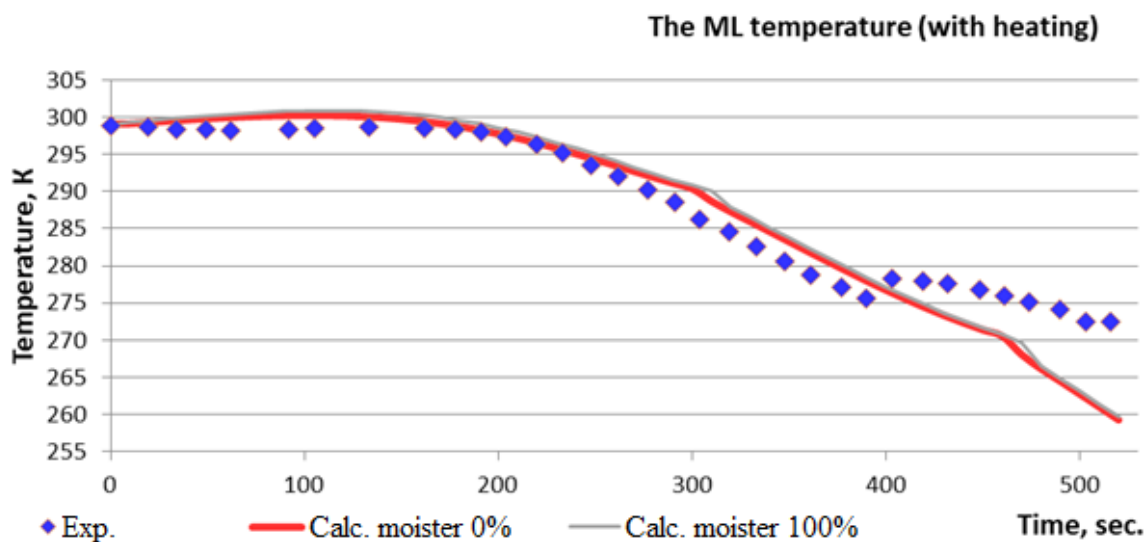
(figures 3, 4) and the pressure in the VC (figures 5, 6) from the time process were obtained. Figure 7 shows the results of ML evaporation at the time, which suggests that during heating, ML begins to evaporate after 200 s and corresponds to the measured values for the residual mass of the ML at the time of freezing.

Figure 8 presents the variation of the VC evacuate pump operation and the total energy of the gas and ML from the time of the process without ML heating. Table 1 shows the comparison of the consumed useful energy from the pump power of 500 W without heating and with ML heating using the rangette power of 3.57 W for pumping air and ML evaporation. The calculations showed that the chances of freezing costs amounted 167179 J and 177146 J, respectively for these two experiments.

In figures 9 and 10 the mass variation and vapour partial pressure in the tub from the time of the process without heating and with heating are shown.



**Figure 3.** The ML temperature dependence on time (without heating).



**Figure 4.** The ML temperature dependence on time (with heating).

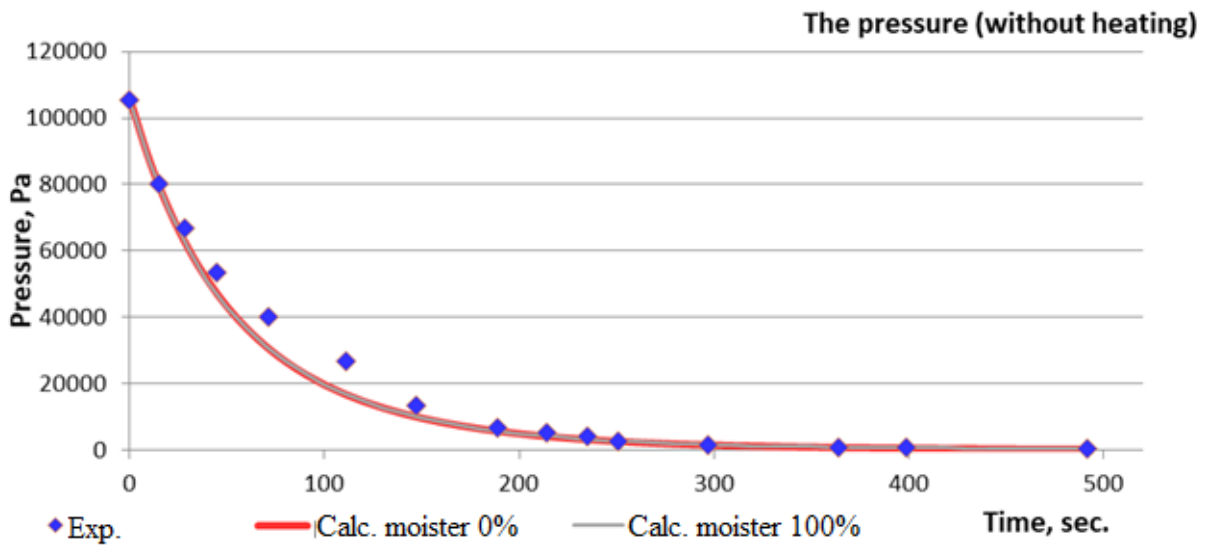


**Figure 5.** The ML pressure dependence on time (without heating).

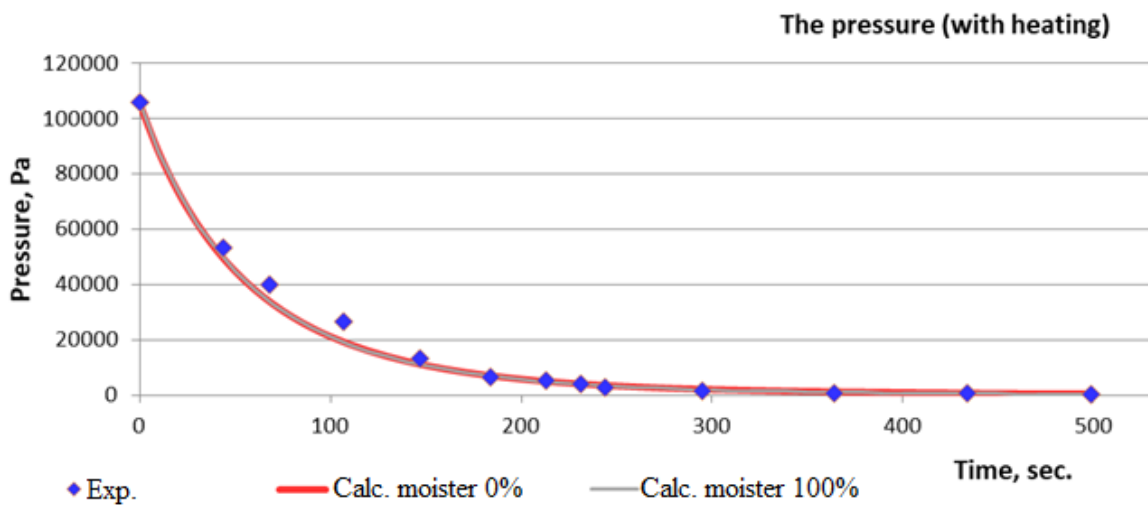


**Figure 6.** The ML pressure dependence on time (with heating).

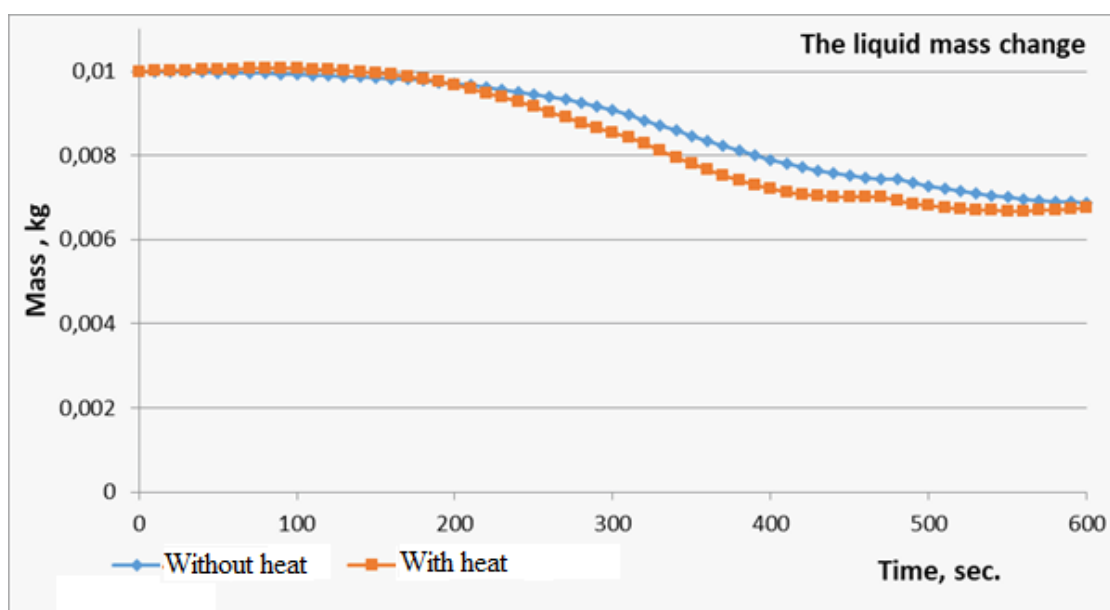


**Figure 7.** The ML mass dependence in EMT on time (without heating and with heating).

**Table 1.** The value of the useful operation of pumping and rangette with an initial moister content of 0% and 100%.

The time $t$ , sec	The amount of pumping operation and ML heating, J.			
	Without heating		Heating – 3.57 W	
	The moister content 0%	The moister content 100%	The moister content 0%	The moister content 100%
100	31427.0	31434.0	29849.0	29854.0
200	77455.0	77457.0	74292.0	74290.0
300	122893.0	122868.0	118665.0	118617.0
400	1672565.0	167175.0	162223.0	162080.0
500	211122.0	210994.0	205009.0	204759.0
600	254880.0	254691.0	243102.0	242328.0

From the results presented in table 1 it follows that the introduction of ML heating leads to a reduction in total energy costs: adding heating energy in the amount of  $\sim 2000$  J was a reduction in total cost of  $\sim 12000$  J.

For the combination of effect parameters (heating and vacuumization), the effect of moister content is not essential.

Thus, there is an optimum ratio of energy consumption for the creation of a vacuum and heating.

To illustrate this phenomenon, an example with the following initial data is provided: to reduce energy consumption in order to pump the air and increase the order of the energy consumption to heat, the quantity of the evaporated liquid increased by three times while reducing the overall energy consumption by six times.

If you enter criteria  $m_w/E_\Sigma = K$ , for the calculation in Table 1 this ratio  $K_1 = 16.37$  g/MJ, and for the latest example  $K_2 = 220.94$  g/(MJ).

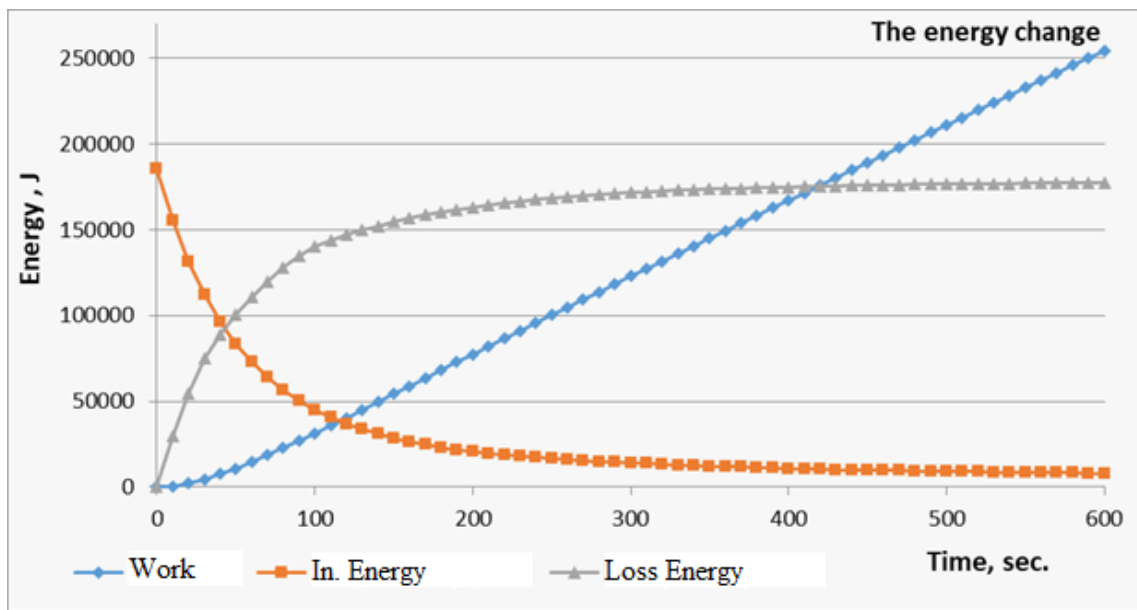


**Figure 8.** The dependence of the work and the total energy of the gas and ML on the time of the process without ML heating.

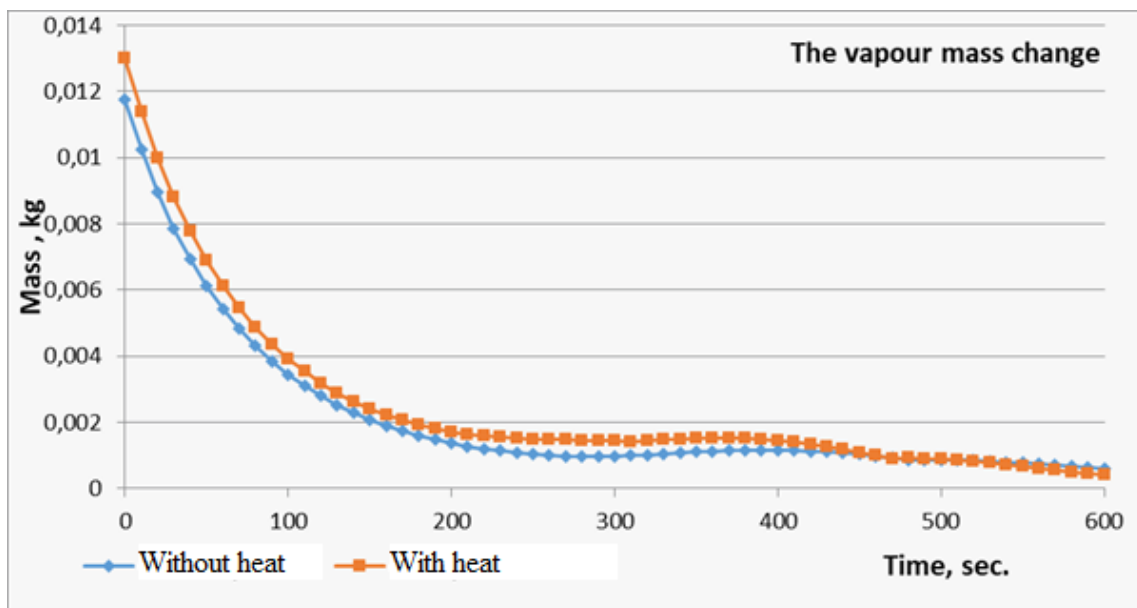


**Figure 9.** The vapour mass dependence in EMT on time (without heating and with heating).

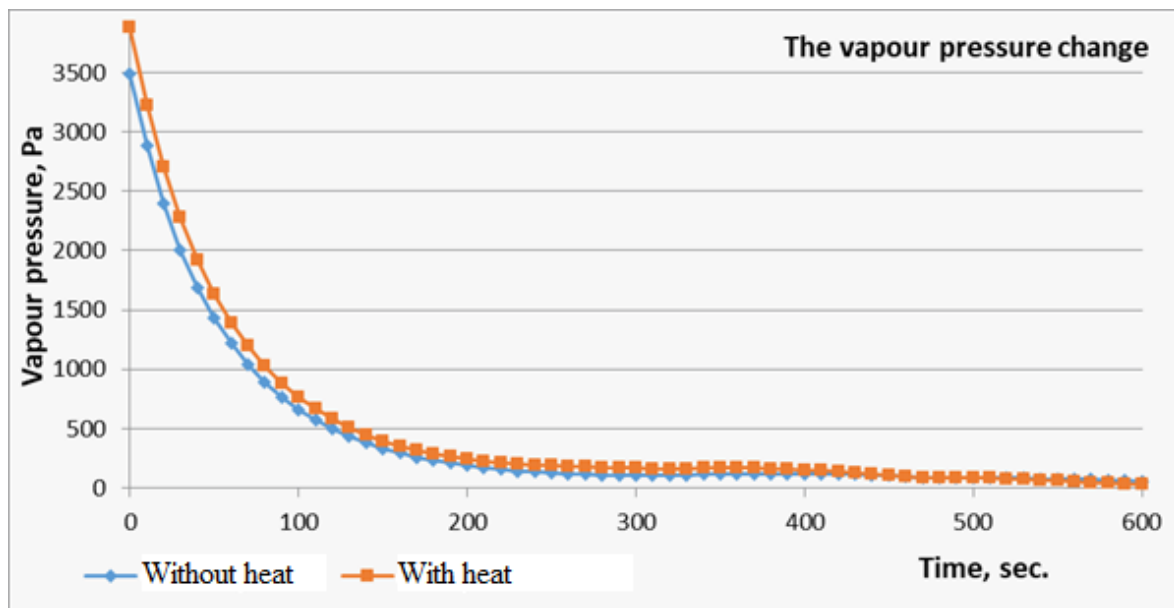


**Figure 10.** The vapour partial pressure dependence in EMT on time (without heating and with heating).

## 7. Results and discussion

The discrepancy between the experimental and calculated results on temperature by 2–3 K after 200 s and the pressure to 15% around 100 s by time can be explained as follows. In numerical simulations, the ML level in the EMT has a uniform thickness, and in the real experiment ML takes uneven thickness with the formation of separate droplets and separate boiling (figure 11, *a*). To 400–440 seconds (without heating and with heating) in the experiment, sometimes there is increased evaporation, followed by the formation of ice (figure 11, *b*). This leads to the release of a certain amount of heat when icing that is observed in the graphs: first, with a sharp decrease in the ML temperature, and then with the subsequent overshoot of increasing it.

In the field of 100 s, there is an increase in pressure resulting from evaporation that is more active. It is also possible to explain the uneven thickness of the ML layer due to the active evaporation and boiling. Where the layer is thinner, evaporation is faster, the pressure increases and the temperature decreases slightly.

In the numerical calculations, this no effect is observed due to the uniform thickness of the ML: The ML value temperature gradually decreases to zero, and pressure – up to 400 Pa. In the experiments and calculations of zero temperature and pressure of 400 Pa onset occurs almost at the same time (~520s).

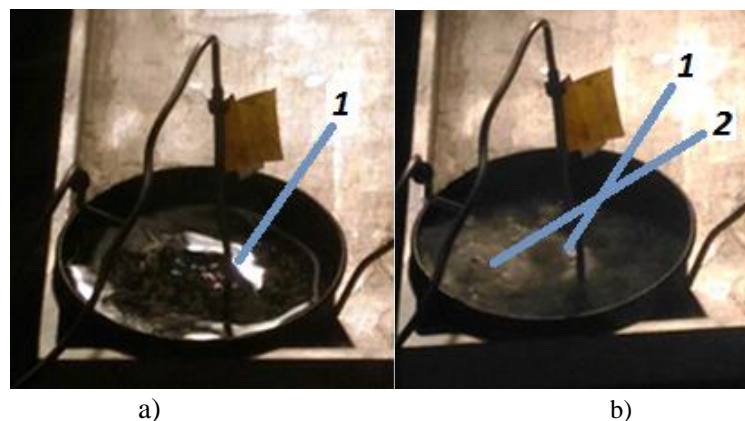


**Figure 11.** Phase transitions of the ML in the EMT during the experiments: *a* – evaporation; *b* – freezing; *1* – is the liquid; *2* – is the ice.

In the experiments without heating, the ML evaporated mass amounted to 2.15 g (21.5% of initial mass). In the experiments with heating, the ML evaporated mass amounted to 2.9 g (29 % of initial mass).

The power expended on the evaporation of a given ML mass, without heating is equal to 86.2 W, while with heating – to 89.6 W.

In both cases (without heating and with heating) at the end of the experiment ML freezing occurred: in the experiment without heating – at 613 Pa and the ML temperature 275 K, and with heating at 573 Pa and the ML temperature 273 K. This is due to the low ML temperature and the reduced pressure in the VC.

Thus, the disadvantage of using vacuum pump for vacuum drying is constant pressure decrease in VC, which leads to ML freezing. The vacuum pump does not control pressure change.

To maintain a constant reduced pressure at a certain level it is proposed to use a vortex tube, the principle of which is based on the Ranque-Hilsch Effect [17]. It is possible to use a counterflow vortex tube, the method of calculation which has been tested in [18].

## 8. Conclusion

1. The mathematical model of the evaporation process of model liquid with the free surface boundary conditions of the "mirror" type in thermal vacuum influences and the numerical estimates of the parameters of evaporation process is developed.
2. The experimental stand, comprising a vacuum chamber, the experimental model tank with heated is developed. Experimental researches were conducted.
3. A comparative analysis of numerical and experimental results showed a close match.
4. The downside of using vacuum pump for ML evaporation is the inability to control the pressure inside the vacuum chamber, so in the future it is suggested to consider a vortex tube for producing a vacuum.

## Acknowledgements

The research was supported by the grant of the Ministry of education and science of the Russian Federation "Improvement of environmental safety and economic efficiency of launch vehicles with main liquid rocket engines", No. 9.1023.2017 PCH

## References

- [1] Kutovoj V 2008 *Device for thermal vacuum drying* Patent Russia no 2315928
- [2] Kutovoj V, Kazarinov Yu, Lucenko A, Nikolaenko A and Koshelnikov V 2014 *Energy saving method for preparation of solid fuel for burning* vol **8** (Energoberezhnie. Energy. Ergoaudit) pp 61–66
- [3] Ermakov S 2007 *Device vacuum drying and method vacuum drying* Patent Russia no 2299385
- [4] Shabetnik G 1998 *Method of vacuum drying of materials and device for vacuum drying of materials* Patent Russia no 2121638
- [5] Kovalev L and Kovaleva N 2007 *Method and device for energy-saving dehydration and drying in vacuum* Patent Russia no 2295681
- [6] Kovalev L and Kovaleva N 2005 *Method of low-temperature vacuum dehydration of materials and device for its implementation* Patent Russia no 2246079
- [7] Gubanok I, Dubinsky V, Egorov I, Posin V, Usenko M and Endeka Yu 2006 *Method of drying of pipelines and device for its implementation* Patent Russia no 2272974
- [8] Naumejko V, Naumejko S and Naumejko A 2007 *Method and device for drying of gas pipelines* Patent Russia no 2300062
- [9] Zhang Z, Zhang Y, Zhao L, Zhang W and Zhao S 2015 Parameter Sensitivity of the Microdroplet Vacuum Freezing Process *Mathematical Problems in Engineering* vol **2** p 8

- [10] Zhang Z, Gao J and Zhang S 2016 Heat and Mass Transfer of the Droplet Vacuum Freezing Process Based on the Diffusion-controlled Evaporation and Phase Transition Mechanism *Scientific Reports* vol **6** p 7
- [11] Du W, Zhao J and Li K 2012 Experimental study on thermal-dynamical behaviours of liquid droplets during quick depressurization *Journal of Engineering Thermophysics* vol **33** pp 1349–1352
- [12] Shin H, Lee Y and Jurng J 2000 Spherical-shaped ice particle production by spraying water in a vacuum chamber *Applied Thermal Engineering* vol **20** pp 439–454
- [13] Frenkel' Ya 1975 *Kinetic theory of liquids* (Moscow: Science) p 592
- [14] Chechyotkin A 1971 *High temperature heat carriers* (Moscow: Energiya) p 496
- [15] Zakharevich A, Velikanov V and Vympin E 2015 The ignition fragment wood heated to a high temperature of the plate *MATEC Web of Conf. Heat and Mass Transfer in the Thermal Control System of Technical and Technological Energy Equipment* (Tomsk) vol 23 p 5
- [16] Panichkin A and Varepo L 2013 Numerical calculation of the free motion of a small volume of viscous incompressible liquid between two rotating cylinders *Computational technologies* vol 2 pp 62–71
- [17] Korkodinov Ya and Hurmatullin O 2012 The Use of the Ranque-Hilsch Effect *Bulletin of Perm national research Polytechnic University* vol 14 pp 42–54
- [18] Kuznetsov V and Makarov V 2016 *Vortex tube: experiment and theory* (Omsk: OmSTU publishing) p 239